# Light scattering of double wall carbon nanotubes under hydrostatic pressure: pressure effects on the internal and external tubes

Pascal Puech, Hannes Hubel, David J. Dunstan, Ayman Bassil, Revathi Bacsa, Alain Peigney, Emmanuel Flahaut, Christophe Laurent, Wolfgang Bacsa

# Light scattering of double wall carbon nanotubes under hydrostatic pressure: pressure effects on the internal and external tubes

**P. Puech**[1], **H. Hubel**[2], **D. J. Dunstan**[2], **A. Bassil**[1], **R. Bacsa**[3], **A. Peigney**[3], **E. Flahaut**[3], **C. Laurent**[3], and **W. S. Bacsa**[*, 1]

[1] Laboratoire Physique des Solides de Toulouse UMR-CNRS 5477, IRSAMC, Université Paul Sabatier, 118 Route de Narbonne, 31062 Toulouse, France
[2] Department of Physics, Queen Mary, University of London, London E1 4NS, UK
[3] CIRIMAT-LCMIET, UMR CNRS 5085, Université Paul Sabatier, 118 Route de Narbonne, 31077 Toulouse cedex 4, France

**PACS** 61.46.+c, 62.50.+p, 63.22.+m, 78.30.Na

We report high-pressure Raman light scattering studies up to 10 GPa on double walled carbon nanotubes using two pressure transmitting media. In alcohol, a clear splitting of the G band is observed up to 10 GPa. This splitting is evidence for both discontinuous tangential stress and continuous radial stress. A structural distortion seems to be present at 3 GPa, revealed by a spectroscopic signature at 1480 $cm^{-1}$. With argon as the pressure transmitting medium, the nanotubes bundles show a transition at 6 GPa which corresponds to a collapse to a flattened structure and removes the splitting. The comparison of the pres-sure coefficients before the transition for the two pressure transmitting media shows that the ratio of the two coefficients associated with internal and external tubes, is the same but the absolute values are differ-ent.

## 1 Introduction

Interest in carbon nanotubes (CNT) has been growing since their discovery in 1991 [1], thanks to their exceptional properties leading to a large number of potential applications [2]. Double wall carbon nanotubes (DWCNT) are more stable than single wall tubes (SWCNT). As the internal tube is protected by the external tube, interaction of the external tube with its environment will to a lesser extend influence the mechanical properties. This will be important for molecular motor applications. The DWCNT can also be considered as a molecular pressure sensor giving information of the interaction of the external tube with adsorbed molecules. We use inelastic light scattering as a tool to examine the mechanical properties of DWCNTs. DWCNTs give the opportunity to explore the effect of hydrostatic pressure on the internal tubes. Multi wall carbon nanotube samples have a large range of diameters and variable number of walls, which makes it difficult to distinguish contributions from internal and external tubes. Double wall carbon nanotubes with narrow diameter distribution have recently become available and contributions from the internal tubes in the Raman spectrum have been identified. There have been a number of reports on multi wall and single wall CNT's under hydrostatic pressure. Tang et al. [3] observed with X-ray a structural distortion near 2 GPa attributed to a faceting of the tube. The X-ray diffraction profile of Sharma et al. [4] shows that the diffraction line related to the tubes vanishes beyond

[*] Corresponding author: e-mail: wolfgang.bacsa@lpst.ups-tlse.fr

~10 GPa. The circular tube section is proposed to be transformed into flattened elliptical shape. A highly flattened structure corresponding to a peanut structure has been predicted by Wu et al. [5]. SWNTs have been probed by Raman spectroscopy and under high pressure extensively [6]. The pressure behaviour of hollow nanostructures [7] as well as multi wall CNTs [8] have been explained using the elastic continuum model. *Ab-initio* [9, 10], molecular dynamics calculations [11], have been used to understand the transition, at low and high pressure. A recent review focussed on Raman spectroscopy on CNTs at high-pressure [6] notes that there is no clear correlation between the observed pressure coefficient in different samples and pressure media. Schlecht et al. [11] have studied isolated single-walled carbon nanotubes under high-pressure and find experimentally an identical frequency dependence of the optical mode in bundled and isolated SWCNTs, which is not predicted by their model simulations using generalized tight-bending molecular dynamics (GTBMD). Venkateswaran et al [12] find using GTBMD, that the van der Waals interaction makes an important contribution to the frequency and pressure coefficient of the radial breathing modes (RBM). The assumption that the pressure-transmitting medium does not penetrate in the tube bundle is inconsistent with the small observed shift of the RBMs of SWCNTs in an alcoholic mixture [13]. It is found that the observed band positions at zero pressure depend on the pressure medium. Wood et al. [14, 15] show that the frequency shift of the D* mode ranges from 2610 to 2630 $cm^{-1}$. The observed shift correlates with the cohesive energy density of the medium. Teredesai et al [16] have observed with SWCNTs a higher-pressure coefficient with water as pressure medium. We have recently explored double wall carbon nanotubes using a methanol-ethanol mixture as pressure medium [17]. Here we compare the Raman spectra under hydrostatic pressure using two different pressure media. We also report on the low and additional high frequency bands.

## 2 Samples and experiment

The DWCNTs were prepared by the catalytic chemical vapour deposition method (CCVD). Selective reduction at 1000 °C in a methane-hydrogen (18% CH4) atmosphere of a solid solution of a transition metal oxide (CoO) and an insulating oxide (MgO) led to the formation of small diameter CNT with one to four walls; for more details see [18, 19]. After the reaction, the not reacted Co and MgO were dissolved in dilute (3.7%) hydrochloric acid and CNT were recovered. High-resolution electron microscopy images showed the presence of individual and small bundles of DWCNTs with radius ranging from 0.3 to 1.5 nm. The tubes were single, double or triple walled with about 80% of DWCNTs and a few four walls tubes. A significant fraction of DWCNTs had internal radius smaller than 0.5 nm. The mean radius is 0.7 nm. All Raman spectra were recorded at room temperature using a microprobe instrument from Renishaw Inc. The scattered light was collected in backscattering geometry using a microscope objective (× 20) to focus the laser beam (633 nm) on to the sample inside the pressure cell. The high-pressure Raman measurements were performed in a diamond anvil cell with a 4 : 1 mixture by volume of methanol-ethanol or argon as the pressure-transmitting medium. The pressure chamber was defined by the volume of a 200 μm diameter hole in a stainless steel gasket (thickness of 100 μm). The pressure was monitored using the luminescence of a ruby chip inside the cell. For the liquid pressure medium, the DWCNTs were dispersed using a ultrasonic bath before loading. With argon, an agglomerated tube sample was placed in the drilled hole of the gasket before cryogenic loading of argon. We have used for both experiments samples from the same batch of DWNTs.

## 3 Experimental results

Figure 1 shows the Raman spectra as a function of applied pressure in the high frequency range obtained using the methanol-ethanol pressure medium. We observe a splitting of the G band, the in-plane optical zone centre phonon mode of graphite. A broader band is located at 1480 $cm^{-1}$. The splitting can be attributed to the internal and external tubes as will be shown below. The higher frequency band is attributed to the external walls and the low frequency band to the internal walls. The fitted band positions are shown as a function of applied pressure in Fig. 2. Figure 3 shows spectra recorded on different locations

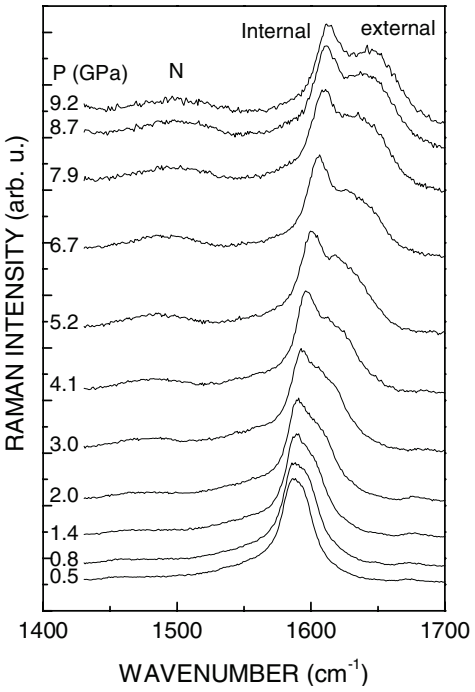


**Fig. 1** Raman spectra of the G band region with methanol-ethanol as pressure-transmitting medium.

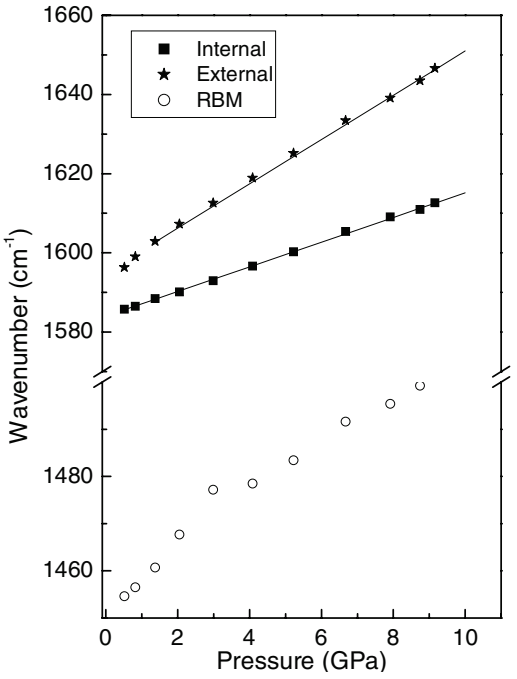


**Fig. 2** Variation of the frequency as a function of pressure. Pressure-transmitting medium is methanol-ethanol.

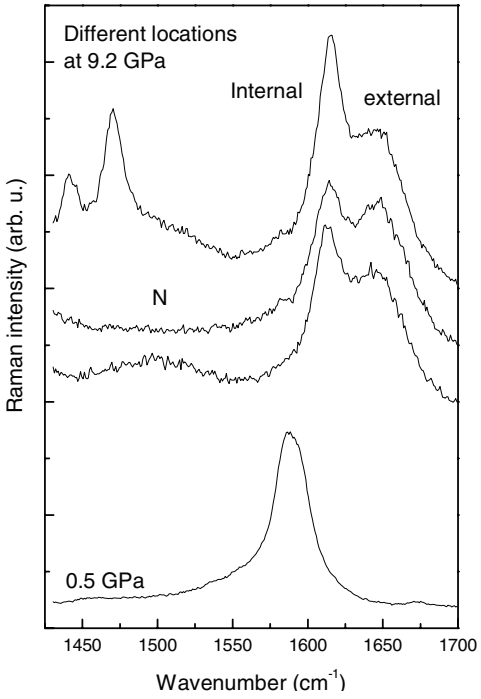


**Fig. 3** Correlation between the peak located near 1480 $cm^{-1}$ and the peak associated to the external tubes. Pressure-transmitting medium is methanol-ethanol.

in the pressure cell. We can see a correlation between the relative intensity of one of the bands in the doublet and the appearance of the broader band at 1480 $cm^{-1}$. The intensity of the band at 1480 $cm^{-1}$ is larger when the intensity of the band associated to the external walls is smaller. The band at 1480 $cm^{-1}$ has been report in the literature [20] and attributed to tubes with a larger number of defects. We note that the intensity of the band associated to the internal tube does not change. In Fig. 2 we see that at low pressure, the frequency of the external walls does not follow the same linear behaviour obtained at higher pressures (>3 GPa).

The transition at 3 GPa observed with the alcohol medium is unusual. More measurements will be needed to clarify the behaviour in this range. The pressure coefficient changes near 3 GPa. Below 3 GPa the pressure coefficient is in range of 10 $cm^{-1}$/GPa while at higher pressures the pressure coefficient reduces to 5.6 $cm^{-1}$/GPa. The band associated to the internal walls follows linear pressure dependence at low and high pressures. Differences between the internal and external walls are also observed in the behaviour of the line-width with applied pressure. The line-width of the band associated to the internal tube is constant while the line-width of the band of the external walls increases linearly up to 6 GPa and saturates at higher pressures. In the low frequency range we have observed the RBMs located at 220 $cm^{-1}$ and 260 $cm^{-1}$ up to 6 GP. A band located at 340 $cm^{-1}$ persisted to higher pressures. The origin of this band is not yet understood. It was attributed to a second harmonic of RBM [21]. But Venkateswaran et al. [22] shows that this explanation cannot fully explain the frequency shift of this peak with applied pressure. The frequency shift is too small and persists also with argon as pressure medium. At the highest pressure applied the frequency shift of the G band of the external walls approaches ~50 $cm^{-1}$. This is the same value observed for single wall CNTs [8].

In Fig. 4 we show the Raman spectra obtained using argon as the pressure-transmitting medium. Cryogenic loading does not permit to obtain values at low pressures. When releasing the pressure some spec-

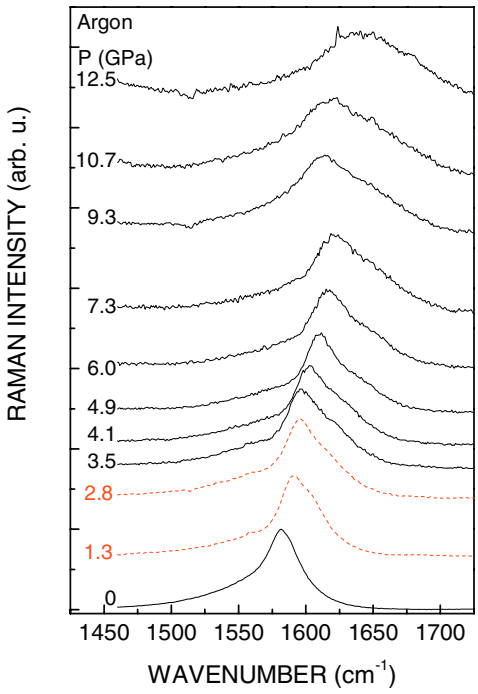


**Fig. 4** Raman spectra associated to the G-band. Notice a decrease of the frequency at 9.3 GPa. The dotted spectra are recorded while reducing the pressure. Pressure-transmitting medium is argon.

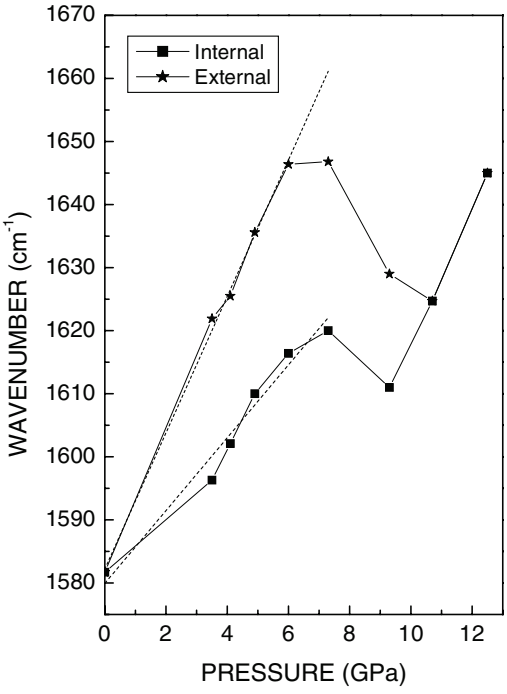


**Fig. 5** Variation of the G-band frequency as a function of the pressure. The pressure-transmitting medium is argon.

tra at low pressure have been recorded and are shown as dotted lines. Fully hydrostatic conditions are probably not established when releasing pressure, leading to uncertainties on the pressure calibration. We will not use them in the following analysis. We have used non-linear least square fitting to determine the peak positions as a function of applied pressure (Fig. 5). The frequency shift is larger in the 3–6 GPa pressure range with the alcohol mixture as pressure transmitting medium. We find a pressure coefficient for the internal tube of $6 \pm 1$ cm$^{-1}$/GPa and for the external tube of $10 \pm 1$ cm$^{-1}$/GPa. When the frequency shift associated to the external walls reaches 60 cm$^{-1}$, a transition is observed. This high pressure induced frequency shift was not obtained with the alcoholic mixture. After the pressure-induced transition, the frequencies decrease and the splitting of external and internal walls disappears. When increasing the pressure furthermore the pressure coefficient is linear and the frequency shift is close to 45 cm$^{-1}$ at 10 GPa. When decreasing the pressure, the splitting is recovered, showing a reversible transition.

## 4 Discussion

We first discuss the splitting of the G-band with applied pressure for double wall tubes. While the phase transition in SWCNTs has been identified as deformation of the cylinder shape, the presence of the internal wall is expected to reduce the deformations. Tight binding model simulations and local density approximation calculations confirm the consistency of the elastic continuum shell model [23]. In order to explain the lower pressure coefficient of the internal tube in DWCNTs, we have used the elastic continuum shell model [7, 8, 24]. For the pressure dependence of a single shell with a finite wall width we obtain the following expressions for the elements of the strain tensor:

$$\sigma_{rr} = -A\left(1-\frac{B}{r^2}\right), \qquad \sigma_{\theta\theta} = -A\left(1+\frac{B}{r^2}\right) \quad \text{and} \quad \sigma_{zz} = -A\ , \tag{1}$$

$A$ and $B$ are constants which depend on the boundary conditions. We consider two separate cylinders by introducing a discontinuity of the tangential stress component and use a continuous radial stress component. We write for the pressure external $-p(R_2)$, between the tube $-pi(R_i)$ and zero at the inside. We obtain two parameters for $A$ and $B$ for the internal and external tube. For the external tube we obtain:

$$A_{\text{ext}} = \frac{R_2^2 p - R_i^2 p_i}{R_2^2 - R_i^2} \quad \text{and} \quad B_{\text{ext}} = \frac{p - p_i}{\dfrac{p}{R_i^2} - \dfrac{p_i}{R_2^2}} \tag{2}$$

and for the internal tube:

$$A_{\text{int}} = \frac{R_i^2}{R_i^2 - R_1^2} p_i \quad \text{and} \quad B_{\text{int}} = R_1^2\ , \tag{3}$$

$p_i$ is obtained by minimizing the elastic strain energy.

$$p_i = \frac{\dfrac{R_2^2}{R_2^2 - R_i^2}(5-4\nu)}{3\left[R_i^2\left(\dfrac{1}{R_2^2 - R_i^2} + \dfrac{1}{R_i^2 - R_1^2}\right)\right](1-2\nu) + 2\left(\dfrac{R_2^2}{R_2^2 - R_i^2} + \dfrac{R_1^2}{R_i^2 - R_1^2}\right)(1+\nu)} p\ . \tag{4}$$

By using the derived expressions for the constants $A$ and $B$ for the external and internal walls for the tangential stress component, we find that the high frequency G-band can be attributed to the external tubes and the low frequency G-band to the internal tubes. When looking at the diameter dependence of the coefficients $A$ and $B$ we find that the tangential stress is nearly independent for the internal tube but varies linearly for the external tube for the diameter range found in our sample (0.5–1.5 nm) [17]. Con-

sequently, we associate a inhomogeneous broadened of the band of the external tube with applied pressure with the diameter distribution.

When taking argon as a pressure-transmitting medium we observe a transition at 6 GPa. A similar pressure induced transition has been observed for SWCNTs at 10 GPa using an alcohol pressure-transmitting medium [25]. In both cases, the transition occurs with a frequency shift of the G-band at 60 $cm^{-1}$. Single as well as double wall tubes have the same pressure coefficient after the transition. This rules out effects due to tube faceting. It is more likely that the tubes are flattened. The flattening has been predicted by recent *ab-initio* calculations [10] and also observed for hollow nanostructures [7].

The fact that the pressure coefficient depends on the pressure medium suggests that the interaction of the pressure medium with the tube is not negligible. It has been noted in the literature that CNTs are sensitive to molecular pressure. Wood et al. [14, 15] have shown that CNTs can be considered as a molecular sensor of the medium. By immersing SWCNT in a variety of liquids and dispersing them using ultrasound, they observe a frequency shift of the D* Raman peak up to 20 $cm^{-1}$ in water compared with the values observed in air. Teresdai et al. [16] have observed for SWNTs using two different pressure transmitting media, alcohol mixture and water, that the pressure coefficient is different. The pressure coefficient is higher in water (7 $cm^{-1}$/GPa) as compared to alcohol (6 $cm^{-1}$/GPa). No helium, neon or argon transmitting pressure media has been reported to our knowledge so far. Model simulations [12] suggest that no fluid is likely to be present between CNT bundles. All the pressure coefficients are similar in the low-pressure range (0–3 GPa). Above this range a change in the pressure coefficient is observed in the case of alcohol. This change is not related to a shape change. The RBMs are not influenced. At the high-pressure transition, all the shifts induced by pressure are reduced. This reduction is somewhat higher for alcohol than when water is added in the alcohol mixture [16]. We can advance two explanations: faceting or polygonalization [3] of the external tube resulting in a modified pressure coefficient. Small distortion of the circular cross section might preserve the splitting of the G-band. This would imply local non-hydrostatic pressure conditions. The second explanation takes into account of the interaction of the pressure medium with the CNTs. A local organization of the pressure medium can form a concentric shell around the tube, which has the consequence to reduce the pressure on the tube in the same manner as the internal tube experiences a smaller pressure than the external tube.

## 5 Conclusion

DWCNTs give the opportunity to distinguish pressure induced spectral changes from internal and external walls in multi wall carbon nanotubes. A first low-pressure transition is observed at 3 GPa in alcoholic mixture, which could correspond to a structural distortion or to an interaction with the medium. Further experiments are needed to elucidate this point. When the G-band frequency of the outer tube shifts by 50–60 $cm^{-1}$, a collapse of the cylindrical structure is observed which reduces the pressure-induced shifts and removes the G-band splitting. The pressure transitions are reversible. The splitting of the G-band reappears when releasing the pressure. The splitting of the G-band can be explained by considering a tangential discontinuity of the stress component as one goes from the external wall to the internal tube. The ratio of the pressure coefficient of internal and external walls remains the same independent of the medium.

## References


[1] S. Iijima, Nature (London) **354**, 56 (1991).
[2] S. Reich, C. Thomsen, and J. Maultzsch, Carbon Nanotubes: Basic Concepts & Physical Properties (Wiley-VCH, Weinheim, 2004).
[3] J. Tang, L. C. Qin, T. Sasaki, M. Yudasaka, A. Matsushita, and S. Iijima, Phys. Rev. Lett. **85**, 1887 (2000).
[4] S. M. Sharma, S. Karmakar, S. K. Sikka, P. V. Teredesai, A. K. Sood, A. Govindaraj, and C. N. R. Rao, Phys. Rev. B **63**, 205417 (2001).
[5] J. Wu, J. Zang, B. Larade, H. Guo, X. G. Gong, and F. Liu, Phys. Rev. B **69**, 153406 (2004).
[6] I. Loa, J. Raman Spectrosc. **34**, 611 (2003).

[7] J. Sandler, M. S. P. Shaffer, A. H. Windle, M. P. Halsall, M. A. Montes-Moran, C. A. Cooper, and R. J. Young, Phys. Rev. B **67**, 035417 (2003).
[8] C. Thomsen, S. Reich, H. Jantoljak, I. Loa, K. Syassen, M. Burghard, G. S. Duesberg, and S. Roth, Appl. Phys. A **69**, 309 (1999).
[9] T. Yildirim, O. Gulseren, C. Kilic, and S. Ciraci, Phys. Rev. B **62**, 12648 (2000).
[10] S. P. Chan, W. L. Yim, X. G. Gong, and Z. F. Liu, Phys. Rev. B **68**, 075404 (2003).
[11] U. Schlecht, U. D. Venkateswaran, E. Richter, J. Chen, R. C. Haddon, P. C. Eklund, and A. M. Rao, J. Nanosci. Nanotechnol. **3**, 139 (2003).
[12] U. D. Venkateswaran, A. M. Rao, E. Richter, M. Menon, A. Rinzler, R. E. Smalley, and P. C. Eklund, Phys. Rev. B **59**, 10928 (1999).
[13] A. K. Sood, P. V. Teredesai, D. V. S. Muthu, R. Sen, A. Govindaraj, and C. N. R. Rao, phys. stat. sol. (b) **215**, 393 (1999).
[14] J. R. Wood and H. D. Wagner, Appl. Phys. Lett. **76**, 2883 (2000).
[15] J. R. Wood, Q. Zhao, M. D. Frogley, E. R. Meurs, A. D. Prins, T. Peijs, D. J. Dunstan, and H. D. Wagner, Phys. Rev. B **62**, 7571 (2000).
[16] P. V. Teredesai, A. K. Sood, S. M. Sharma, S. Karmakar, S. K. Sikka, A. Govindaraj, and C. N. R. Rao, phys. stat. sol. (b) **223**, 479 (2001).
[17] P. Puech, H. Hubel, D. Dunstan, R. R. Bacsa, C. Laurent, and W. S. Bacsa, Phys. Rev. Lett., accepted for publication (2004).
[18] R. R. Bacsa, Ch. Laurent, A. Peigney, W. S. Bacsa, Th. Vaugien, and A. Rousset, Chem. Phys. Lett. **323**, 566 (2000).
[19] E. Flahaut, R. Bacsa, A. Peigney, and Ch. Laurent, Chem. Commun. **12**, 1442 (2003).
[20] A. Jorio, M. A. Pimenta, A. G. Souza Filho, R. Saito, G. Dresselhaus, and M. S. Dresselhaus, New J. Phys. **5**, 139 (2003).
[21] L. Grigorian, K. A. Williams, S. Fang, G. U. Sumanasekera, A. L. Loper, E. C. Dickey, S. J. Pennycook, and P. C. Eklund, Phys. Rev. Lett. **80**, 5560 (1998).
[22] U. D. Venkateswaran, E. A. Brandsen, M. E. Katakowski, A. Haruntyunyan, G. Chen, A. L. Loper, and P. C. Eklund, Phys. Rev. B **65**, 054102 (2002).
[23] S. Reich, C. Thomsen, and P. Ordejon, Phys. Rev. B **65**, 153407 (2002).
[24] A. P. Boresi and R. J. Schmidt, Advanced Mechanics of Materials, 6th ed. (John Wiley and Sons, New York, 2003), chap. "The Thick-Wall Cylinder".
[25] P. V. Teredesai, A. K. Sood, D. V. S. Muthu, R. Sen, A. Govindaraj, and C. N. R. Rao, Chem. Phys. Lett. **319**, 296 (2000).